Check for updates

# Singlet and triplet energy transfer dynamics in self-assembled axial porphyrin–anthracene complexes: towards supra-molecular structures for photon upconversion†

Victor Gray, [ID] Betül Küçüköz, [ID] Fredrik Edhborg, Maria Abrahamsson, [ID] Kasper Moth-Poulsen [ID] and Bo Albinsson [ID] *

Energy and electron transfer reactions are central to many different processes and research fields, from photosynthesis and solar energy harvesting to biological and medical applications. Herein we report a comprehensive study of the singlet and triplet energy transfer dynamics in porphyrin–anthracene coordination complexes. Seven newly synthesized pyridine functionalized anthracene ligands, five with various bridge lengths and two dendrimer structures containing three and seven anthracene units, were prepared. We found that triplet energy transfer from ruthenium octaethylporphyrin to an axially coordinated anthracene is possible, and is in some cases followed by back triplet energy transfer to the porphyrin. The triplet energy transfer follows an exponential distance dependence with an attenuation factor, $\beta$, of 0.64 Å$^{-1}$. Further, singlet energy transfer from anthracene to the ruthenium porphyrin appears to follow a $R^6$ Förster distance dependence. Porphyrin–anthracene complexes are also used as triplet sensitizers for triplet–triplet annihilation (TTA) based photon upconversion, demonstrating their potential for photophysical and photochemical applications. The triplet lifetime of the complex is extended by the anthracene ligands, resulting in a threefold increase in the upconversion efficiency, $\Phi_{UC}$ to 4.5%, compared to the corresponding ruthenium porphyrin–pyridine complex. Based on the results herein we discuss the future design of supra-molecular structures for TTA upconversion.

Porphyrins, the heterocyclic 18 π-electron conjugated system common in many natural and biological systems, and their related structures are widely studied. In nature, they are essential for light harvesting, energy and electron transfer reactions, catalysis and oxygen transport.[1–3] Accordingly, scientists have studied porphyrin compounds and developed numerous model systems to understand and exploit these versatile and useful compounds. A variety of uses have been explored, such as: light harvesting antennas for artificial photosynthesis and solar energy conversion devices;[4–12] singlet oxygen sensitizers for photodynamic therapy;[13] wires in molecular electronics;[14–17] and triplet sensitizers for triplet–triplet annihilation based photon upconversion,[18–21] to name a few. In both the natural and man-made systems, understanding the mechanisms of energy and electron transfer reactions is crucial. For example, in plants and photosynthetic bacteria triplet energy transfer (TET) occurs

from the light-absorbing chlorophyll moiety to pendant carotenoids as a way of protecting the biological species against reactive singlet oxygen.[22–24] Engineered photosynthetic systems with increased efficiencies will require even greater oxygen protection, motivating further exploration of TET in model porphyrin donor–acceptor systems.[24] Furthermore, in the development of supramolecular structures designed for photochemical applications, such as triplet–triplet annihilation based photon upconversion[25–27] or photocatalysis[28–30] the delicate balance between energy and electron transfer reactions requires careful tuning.

As part of the ongoing studies of energy and electron transfer reactions in porphyrin donor–acceptor system for various photochemical and electrochemical applications,[4,5,7,24,25,31–44] we present a detailed photophysical study of a series of new, well-defined, self-assembled, axially coordinated ruthenium porphyrin–anthracene donor–acceptor systems. These systems consist of 2,3,7,8,12,13,17,18-octaethylporpyrin ruthenium(II) carbonyl (**RuOEP(CO)**) coordinated axially by five different pyridine functionalized anthracene based ligands with various bridge lengths (8–25 Å) or two different dendrimer ligands with 3–7 monomer units. TET from the porphyrin to the anthracene

*Chalmers University of Technology, Department of Chemistry and Chemical Engineering, Gothenburg, Sweden. E-mail: balb@chalmers.se*

This journal is © the Owner Societies 2018

*Phys. Chem. Chem. Phys.*, 2018, **20**, 7549–7558 | 7549

ligand and singlet energy transfer (SET) in the opposite direction are consequently studied as a function of bridge length, and ligand dendrimer size. Transient absorption spectroscopy and time resolved phosphorescence spectroscopy are combined with steady state techniques to study the energy landscape of the complexes. We find that TET to the ligand extends the triplet lifetime of the complex from 20 μs up to 600 μs. With an extended triplet lifetime the sensitization capabilities are improved and we employ the complexes as sensitizers for sensitized triplet–triplet annihilation photon upconversion (TTA-UC). Aiming towards efficient TTA-UC materials in the solid state we further discuss the capabilities of these complexes as sensitizers in supra-molecular TTA-UC systems. As such, this comprehensive study of anthracene–porphyrin complexes unravels important design principles for supra-molecular systems achieving efficient energy transfer.

# 1 Results and discussion

## 1.1 Ligand design and synthesis

Ligand design is based on our previous work with 9,10-diphenyl-anthracene (DPA) based ligands and dendrimeric structures.[25,45] Fig. 1 shows the structures of the ligands: ligand **1** has a *meta*-pyridine substitution, ligands **2–5** have *para*-pyridine substitutions with increasing bridge lengths and dendrimeric ligands **6** and **7** have an increasing number of DPA monomer units. Fig. 1 also shows the structure of the triplet sensitizer octaethyl-porphyrin ruthenium(II) carbonyl (**RuOEP(CO)**).

The synthesis of ligands **1–5** was reported previously.[25] The dendrimer ligands were synthesized by repeating a sequence of three high yielding and simple reactions; bromination followed

by borylation followed by a Suzuki-coupling, similar to our previously established route for DPA dendrons and dendrimers.[45] The synthetic route is illustrated in Fig. S1 and described in more detail in the ESI.† Similar to what was reported previously **RuOEP(CO)** was obtained by refluxing the corresponding free-base porphyrin with $Ru_3CO_{12}$.[46–48] ‡

## 1.2 Binding equilibrium

Upon mixing the porphyrin **RuOEP(CO)** with pyridine (**Pyr**) or the pyridine containing ligands **1–7**, pyridine–porphyrin complexes **RuOEP(CO)L** (L = **1–7** or **Pyr**) are formed. The binding is followed using UV/Vis absorption spectroscopy, as seen in Fig. 2 and Fig. S8 (ESI†). Upon binding to pyridine the porphyrin Q-band absorption is red-shifted[49,50] and the complex Q-band has absorption peaks at 549 and 518 nm.

The pyridine–ruthenium porphyrin bond is very strong, with a binding constant in the order of $10^6$–$10^7$ $M^{-1}$ (ESI,† Table S1), to be compared to the pyridine–zinc porphyrin bond of 6000 $M^{-1}$, reported in our previous work.[25] The larger binding constant leads to about 90% of the ligand being bound to the porphyrin at a 1:1 mixture of **RuOEP(CO)** (total porphyrin concentration is 0.1 mM) and **L** (total ligand concentration is 0.1 mM). To form significant amounts of the zinc porphyrin–pyridine ligand complexes large excess of the ligand is required. The ruthenium based complexes are therefore better suited for fundamental studies since well-defined complexes can easily be formed.

## 1.3 Triplet energy transfer and phosphorescence quenching

**RuOEP(CO)Pyr** is slightly phosphorescent in degassed toluene solutions, Fig. S9 (ESI†), with a quantum yield ($\Phi_P$) of 0.68%. From the phosphorescence onset the triplet state energy $^3$**RuOEP(CO)Pyr\*** is estimated to be 1.90 eV (650 nm), corresponding to a singlet–triplet excited state splitting of 0.35 eV.

The triplet energy of the anthracene ligands is expected to be similar to that of DPA, 1.77 eV.[51,52] Therefore, a small driving force for TET from the porphyrin to the anthracene ligand exists. A common way of studying TET from phosphorescent porphyrins is by monitoring the phosphorescence quenching of the sensitizer by an acceptor. As can be seen in Table 1 there is only partial quenching of the **RuOEP(CO)L** phosphorescence compared to **RuOEP(CO)Pyr**. At first this low degree of quenching and that all compounds show similar phosphorescence quantum yields might seem surprising; its origin will be discussed in the following paragraph.

Nanosecond resolved transient absorption (TA) and time resolved phosphorescence measurements were both performed to further study the TET process, and the results are summarized in Table 2. The TA spectra of the **RuOEP(CO)L** complexes are found in Fig. 3 and Fig. S10 (ESI†). **RuOEP(CO)Pyr** displays strong $T_1$–$T_n$ excited state absorption (ESA) in the 400–500 nm region and a distinct ground state bleach (GSB) at 520 nm and 550 nm, in accordance with the ground state absorption spectra. Both the ESA and GSB decay with a time constant of 20 μs, in accordance with the phosphorescence decay, *vide infra*.
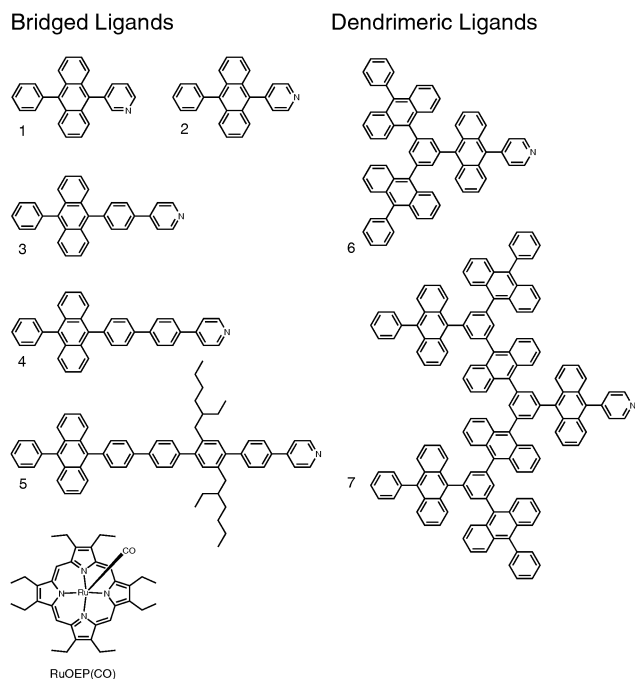


**Bridged Ligands**          **Dendrimeric Ligands**

Fig. 1 Structures of the studied anthracene ligands **1–7** and the octa-ethylporphyrin ruthenium(II) carbonyl **RuOEP(CO)**.

‡ **RuOEP(CO)** is a low-spin d-6 complex, with a singlet ground-state.[47]
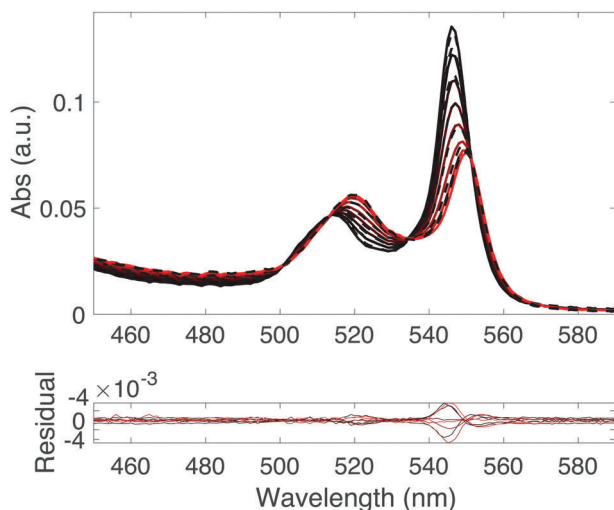
Fig. 2 Shift in **RuOEP(CO)** (0.1 mM) absorption as ligand **1** is added (0–0.1 mM) to form complex **RuOEP(CO)1**. Measured (dashed) and predicted (solid) spectra with residual below. Titration progression from black to red spectra.

Table 1 Phosphorescence quantum yield ($\Phi_p$) of **RuOEP(CO)L** complexes with pyridine (**Pyr**) and ligands **1–7**; triplet energy transfer rates between the ruthenium porphyrin and the ligand; and triplet lifetimes of the ligand ($\tau_{TL}$)[a]

| Ligand | $\Phi_p$ (%) | $k_{TET}$ (s⁻¹) | $k_{bTET}$ (s⁻¹) | $\tau_{TL}$ (μs) |
|---|---|---|---|---|
| **Pyr** | 0.68 ± 0.10 | — | — | — |
| **1** | 0.29 ± 0.07 | $> 10 \times 10^9$ | $> 2 \times 10^8$ | 680 |
| **2** | 0.29 ± 0.01 | $3.6 \times 10^7$ | $7.3 \times 10^5$ | 735 |
| **3** | 0.29 ± 0.01 | $7.6 \times 10^5$ | $2.1 \times 10^4$ | 500 |
| **4** | 0.30 ± 0.05 | $8.4 \times 10^4$ | $1.7 \times 10^3$ | 190 |
| **5** | 0.42 ± 0.12 | $3.3 \times 10^4$ | $0.2 \times 10^3$ | 315 |
| **6** | 0.19 ± 0.01 | $3.7 \times 10^7$ | $3.4 \times 10^5$ | 820 |
| **7** | 0.11 ± 0.01 | $3.8 \times 10^7$ | $2.4 \times 10^5$ | 610 |

[a] Phosphorescence quantum yields, $\Phi_p$ determined in degassed toluene relative to Cresyl violet in methanol. $k_{TET}$ is the triplet energy transfer (TET) rate, $k_{bTET}$ is the rate of back TET and the intrinsic lifetime of the ligand is $\tau_{TL} = k_{TL}^{-1}$.

Table 2 Decay times of **RuOEP(CO)L** in degassed toluene determined from transient absorption (TA)[a] and phosphorescence (p)[b] decays

| Ligand | $\tau_1^{TA}$ (μs) | $\tau_1^p$ (μs) | $\tau_2^{TA}$ (μs) | $\tau_2^p$ (μs) |
|---|---|---|---|---|
| **Pyr** | 20 | 17 | — | — |
| **1** | <0.0001 | — | 400 | 320 |
| **2** | 0.027 | — | 430 | 510 |
| **3** | 1 | — | 310 | 290 |
| **4** | 7 | 7 | 170 | 240 |
| **5** | 12 | 15 | 300 | — |
| **6** | 0.027 | — | 600 | 270 |
| **7** | 0.027 | — | 520 | 190 |

[a] Excited at 550 nm and monitored at 440 nm and 520 nm. [b] Excited at 405 nm and emission monitored at 650 nm.

With the pyridine anthracene ligand **2** the ground state bleach decays with $\tau$ = 27 ns, Table 2, as does the strong porphyrin T₁–T$_n$ ESA, which decays into a longer lived ($\tau$ = 430 μs), weaker ESA in the same 400–500 nm region. This weaker ESA feature corresponds to the T₁–T$_n$ transition of the anthracene unit. The fast

decay of the porphyrin centered triplet followed by the observation of an excited anthracene triplet suggest that there is efficient TET from the porphyrin to the ligand; $^3$**RuOEP\*(CO)L** → **RuOEP(CO)**$^3$**L\***. For anthracene ligands with longer bridges the $^3$**RuOEP\*(CO)L** triplet decays slower, Fig. 3 and Fig. S10 (ESI†), indicating a slower TET, as expected by the exponential distance dependence of TET.[36,37,40]

For the larger dendrimeric ligands, **6** and **7**, the porphyrin triplet also decays in about 27 ns, the same as for **2**, Fig. S10 (ESI†). As the shortest porphyrin–anthracene distance is expected to be the same in these three complexes, the TET rate is expected to be similar. The observed longer decay time increases slightly in the larger ligands, from 430 μs to 600 μs and 520 μs for **2**, **6** and **7**, respectively. Ligand **1**, with a *meta*-pyridine, displays the fastest decay of the porphyrin triplet, faster than the time-resolution of our TA setup. The expected tilted binding in **RuOEP(CO)1** most likely increases the orbital overlap between the porphyrin triplet, located on the ring π-system, and the anthracene unit, explaining the increased TET rate.

Since the TET is only slightly exergonic in the studied systems (∼0.13 eV) it is also possible for TET back (bTET) from the anthracene ligand to the porphyrin to occur; **RuOEP(CO)**$^3$**L\*** → $^3$**RuOEP\*(CO)L**. In other words, the two states could be in equilibrium; $^3$**RuOEP\*(CO)L** ⇌ **RuOEP(CO)**$^3$**L\***. To obtain the actual TET rate, both the forward and backward TET must be considered when analysing the biexponential decays obtained from the TA-measurements. Eqn (1) and (2) describe the relationship between the observed decay times $\tau_1$ and $\tau_2$ (Table 2) with the rate of TET and bTET, respectively:

$$k_{TET} = \frac{k_{TP}\left(\tau_1^{-1} + \tau_2^{-1} - k_{TP}\right) - \tau_1^{-1}\tau_2^{-1}}{k_{TP} - k_{TL}}, \quad (1)$$

$$k_{bTET} = \frac{-k_{TL}\left(\tau_1^{-1} + \tau_2^{-1} - k_{TL}\right) + \tau_1^{-1}\tau_2^{-1}}{k_{TP} - k_{TL}}, \quad (2)$$

where $k_{TP}$ and $k_{TL}$ are the intrinsic triplet decay rates of the porphyrin and ligand, respectively. Eqn (1) and (2) can be derived from the set of coupled rate equations governing the system.[53] A modified expression for the phosphorescence quantum yield, $\Phi_p$, is obtained considering TET and bTET, as described in the ESI.† Assuming an intersystem crossing yield of unity for **RuOEP(CO)L**,[54] the phosphorescence quantum yield is given by eqn (3):

$$\Phi_p = \frac{k_r}{k_{TP} + k_{TET} - k_{bTET} \times \dfrac{k_{TET}}{k_{TL} + k_{bTET}}} \quad (3)$$

where $k_{TP}$ and $k_{TL}$ are the intrinsic triplet decays of the porphyrin and anthracene ligand, respectively. For the derivation of eqn (3) the reader is referred to the ESI.† Combining eqn (1)–(3) one can calculate $k_{TET}$, $k_{bTET}$ and $k_{TL}$. The obtained rates for TET and bTET can be found in Table 1 together with the intrinsic triplet lifetimes of the ligands, $\tau_{TL} = k_{TL}^{-1}$.

For the shortest bridges the effect of bTET is small and $k_{TET}$ is similar to $\tau_1^{-1}$. In complexes with larger donor–acceptor separation the TET and bTET are slower, and the effect of bTET
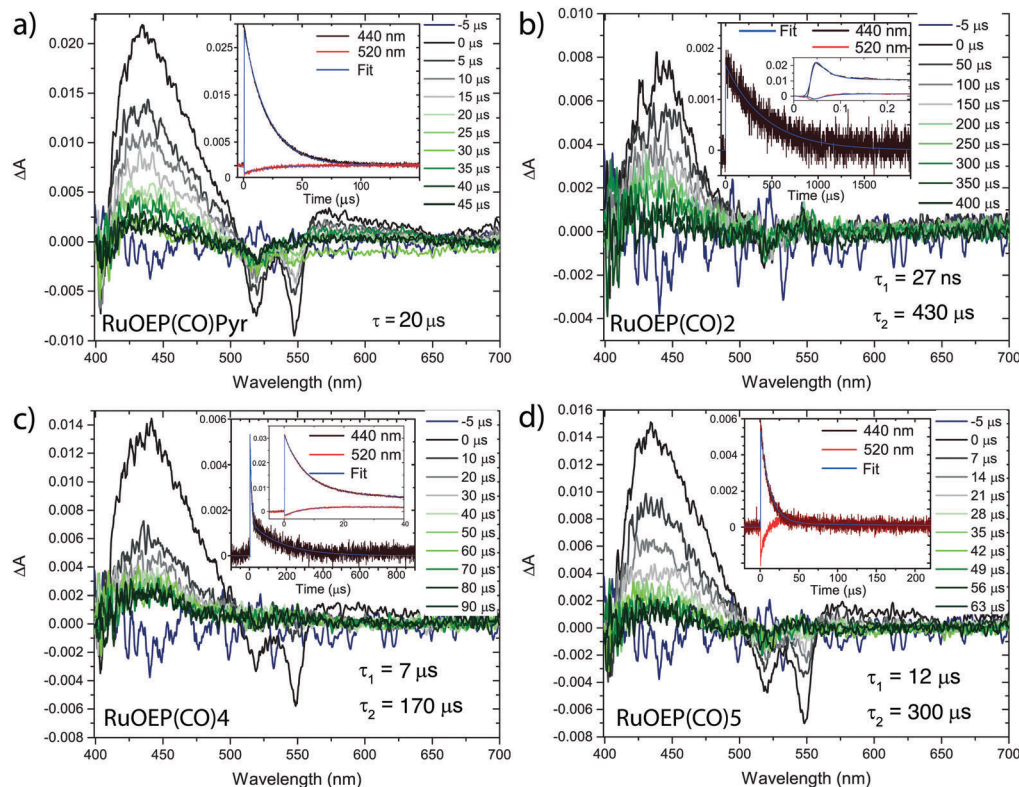
Fig. 3 Transient absorption spectra of (a) **RuOEP(CO)Pyr**, (b) **RuOEP(CO)2**, (c) **RuOEP(CO)4** and (d) **RuOEP(CO)5**. All samples excited at 550 nm in degassed toluene.

is larger. Due to microscopic reversibility the rate $k_{bTET}$ is related to $k_{TET}$ through the Boltzmann factor as described in eqn (4):

$$k_{bTET} = k_{TET} \exp\left(\frac{-\Delta E}{k_b T}\right), \tag{4}$$

where $k_b$ is the Boltzmann constant, $T$ is the temperature and $\Delta E$ is the free energy difference between the triplet states of **RuOEP(CO)** and **L**, estimated spectroscopically to be 0.13 eV (*vide supra*). From the obtained rates we can alternatively estimate the energy splitting to 0.11 eV, in good agreement with that estimated above.

Furthermore, the energy transfer dynamics were also monitored for some of the samples using time-resolved phosphorescence, Table 2 and Fig. S11 (ESI†). In µs emission measurements, the donor only complex, **RuOEP(CO)Pyr**, displays a phosphorescence decay of 17 µs, comparable to that observed for the triplet decay in the TA measurements, Table 2. In the donor–acceptor complexes where the TET is below the time-resolution of our phosphorescence measurements only a longer lifetime is observed, supporting that bTET occurs resulting in the observed delayed phosphorescence. The dendrimeric ligand complexes **RuOEP(CO)6** and **RuOEP(CO)7** also show mono exponential delayed phosphorescence lifetimes. In complexes **RuOEP(CO)4** and **RuOEP(CO)5**, however, a biexponential decay is observed and in both cases the shorter of the two lifetimes are in good agreement to the TET rate determined from TA measurements. The longer lifetime is again longer than the donor only complex,

further supporting bTET as an explanation to the minor phosphorescence quenching. The magnitude of the long lifetimes agrees well between experiments, there is however some discrepancy between the exact lifetimes in the different experiments. One reason can be that in nanosecond TA spectroscopy the long lived ligand state is directly probed and its decay is accurately monitored. In the phosphorescence measurements, on the other hand, the emissive porphyrin triplet state is monitored and the long lived ligand state is thus monitored indirectly. Therefore, the long lived component is expected to only make up a few percent of the total decay making it difficult to measure with the same accuracy.

Fig. 4 shows the dependence of the TET rate as a function of donor–acceptor distance, $R_{DA}$. Since TET processes proceed through an electron exchange mechanism an exponential distance dependence is expected:[36,37]

$$k_{TET} = k_0 \exp(-\beta R_{DA}) \tag{5}$$

where $k_0$ is the rate of TET at zero donor–acceptor separation and $\beta$ is an attenuation factor. Here $R_{DA}$ is defined as the distance between the anthracene core and the porphyrin metal centre obtained from optimized structures of the **RuOEP(CO)2**–**RuOEP(CO)5** complexes.§ For the three complexes with the shortest separation (**RuOEP(CO)L**, **L** = 2–4) $k_{TET}$ decreases

§ Optimized structures of the **RuOEP(CO)L** coordination complexes were modelled with PM3 as implemented in the HyperChem 8.0 computational chemistry package.
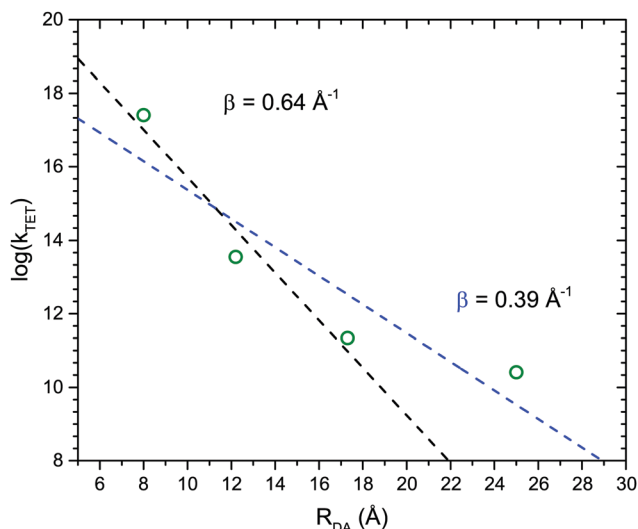
7552 | *Phys. Chem. Chem. Phys.*, 2018, **20**, 7549–7558

This journal is © the Owner Societies 2018

Fig. 4 Triplet energy transfer rates ($k_{TET}$) as a function of donor–acceptor separation ($R_{DA}$) in toluene. The triplet energy transfer rate decreases exponentially with $R_{DA}$, with an attenuation factor $\beta = 0.39$ or $0.64$ Å$^{-1}$, depending on if the longest bridge (**RuOEP(CO)5**, $R_{DA} = 25$ Å) is included in the linear fit or not.
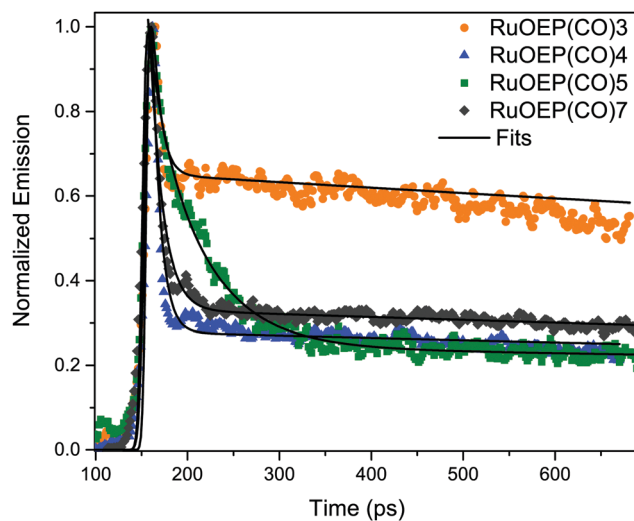


Fig. 5 Fluorescence decays of complexes **RuOEP(CO)L**, where **L** is **3**, **4**, **5** or **7**. Samples excited at 375 nm and decays are the average emission between 415–440 nm.

exponentially with $R_{DA}$ and fits nicely with an attenuation factor $\beta$ of 0.64 Å$^{-1}$. The TET in **RuOEP(CO)5** does not follow this exponential dependence. A possible explanation of the deviation from exponential dependence is the change of the transfer mechanism, from a tunnelling to a hopping mechanism.[55] However, the triplet energy of unsubstituted poly p-phenylene with 5 phenyl units is about 2.3 eV, substantially uphill from the **RuOEP(CO)** triplet state at 1.90 eV.[56] Possibly the disubstitution of 2,6-ethylhexyl on the central phenyl group, the terminal pyridine and the coordination to the ruthenium atom results in a slightly stabilized triplet energy of the bridge enabling hopping. It can, however, not be ruled out that **RuOEP(CO)5** also follows an exponential distance dependence, in that case $\beta$ for the entire series is 0.39 Å$^{-1}$. Including **RuOEP(CO)5** in the analysis results in a worse linear fit, however, 0.39 Å$^{-1}$ and 0.64 Å$^{-1}$ both fall in the range of reasonable $\beta$ values for p-phenylene bridges.[36,57–59]

## 1.4 Singlet energy transfer from anthracene ligands to RuOEP(CO)

Due to the large singlet–triplet splitting in anthracene chromophores, 1.3–1.4 eV, the anthracene ligands function either as triplet acceptors or singlet donors in the studied **RuOEP(CO)L** complexes. Upon complex formation the prompt anthracene emission is quenched by more than 95%, indicating efficient singlet energy transfer (SET) to the porphyrin. Fig. 5 displays the ps-resolved fluorescence decays of complexes with ligands 3–5 and 7; fluorescence decays of ligands with shorter bridges could not be resolved on the current setup. The decays are biexponential, where the fast component is attributed to SET and the longer component to residual emission from unbound ligand. The fraction of the long component in the decay is not directly related to the fraction of unbound species in

the sample, as the lifetime of the free ligand is longer than the repetition rate (80 MHz) a long lived emission signal is built up over time. However, the fact that complexes with ligands **4**, **5** or **7** all have similar fractions of long lived components indicate that the amount of free ligand is similar in all samples, as expected. From the binding constants we estimate that <10% free ligand is present in the samples. The much larger fraction of the long lived component of complex **RuOEP(CO)3** results from the fact that the fast component is shorter than the pulse width. We can still obtain a range of reasonable values for the short component for **RuOEP(CO)3** by expecting a similar fraction of the long lived component and deconvolving the signal with a reasonable pulse width. Further details of the fitting can be found in the ESI.†

The SET in complex **RuOEP(CO)5** occurs with $\tau_{SET} = 48$ ps, Table 3. As expected, shorter bridges exhibit faster SET, $\tau_{SET}$ is about 5 ps for complex **RuOEP(CO)4**. Shortening the bridge further, as in complex **RuOEP(CO)3**, results in a SET that approaches the limit of our time resolution, observed as an increased fraction of the long lived component in the decay. As discussed above we can

Table 3 Ligand fluorescence lifetimes in degassed toluene[a]

| Ligand | $\tau_{SET}$ (ps) | $\tau_0{}^b$ (ns) |
|---|---|---|
| 1 | — | 7.1 |
| 2 | — ($0.1^c$) | 7.1 |
| 3 | 0.5–3 ($0.8^c$) | 4.3 |
| 4 | 5 ± 1 ($5^c$) | 3.8 |
| 5 | 48 ± 2 | 4.0 |
| 6 | — | 5.9 |
| 7 | 8 ± 1 | 5.4 |

[a] $\tau_{SET}$ refers to the quenched lifetime of the anthracene fluorescence in the **RuOEP(CO)L** complex and $\tau_0$ is the unquenched lifetime. [b] Determined for the ligand in separate TCSPC experiments and fixed in the analysis of the shorter lifetimes $\tau_{SET}$. [c] Lifetimes estimated assuming that the singlet energy transfer is solely governed by FRET, they should therefore be considered as an upper limit.

still estimate the SET rate to be between 0.5 and 3 ps by assuming a similar fraction of residual fluorescence as observed in complexes **RuOEP(CO)4**, **RuOEP(CO)5** and **RuOEP(CO)7**. In complexes **RuOEP(CO)1**, **RuOEP(CO)2** and **RuOEP(CO)6** SET is much faster than our time resolution and only the long lived component is observed. It should be pointed out, however, that the steady state emission is quenched almost quantitatively in all complexes. Therefore, the long lived component must arise by residual amounts of unbound ligand, also in complexes **RuOEP(CO)1**, **RuOEP(CO)2** and **RuOEP(CO)6** where the decay component related to SET is not resolved. An interesting observation is that, in the complex with the largest dendrimeric ligand **7**, SET is slowed down compared to the monomer ligand **2** and second generation dendrimer ligand **6**. It indicates that on average the excited singlet state is located further away in the larger structures.

The rate of SET in complexes **RuOEP(CO)L**, with **L** = **3–5**, follows a $R_{DA}^6$ dependence, Fig. S12 (ESI†), indicating that SET is governed by FRET with a Förster distance $R_0 = 50$ Å. Based on the FRET mechanism and taking the spectral overlap between ligand emission and porphyrin absorption into account, the lifetimes can be estimated to 0.1 ps for the shortest bridged ligand **2** in the complex, see the ESI† for details about the calculations. As can be seen in Table 3, the estimated lifetimes for complexes **RuOEP(CO)3**, 0.8 ps, and **RuOEP(CO)4**, 5 ps, are in good agreement with our experimental observations and also confirm that the expected lifetimes in the shortest bridged complex, **RuOEP(CO)2**, are well below our time resolution.

$R_0$ for the **RuOEP(CO)L** complexes is about 10 Å larger than for the corresponding zinc octaethylporphyrin (**ZnOEPL**) complexes, resulting in the SET in the current study being faster compared to similar complexes based on **ZnOEP**.[25] For example, the SET in **RuOEP(CO)5** is three times faster compared to the corresponding zinc complex **ZnOEP5**. The faster SET in the ruthenium complex cannot be explained by the difference in the Förster overlap integral ($J$) as it actually is smaller for the case of the ruthenium complex. One significant difference between the zinc and ruthenium complexes is the ligand binding strength. The Zn–N bond is quite weak ($K_{bind} \sim 10^3$–$10^4$ M$^{-1}$), resulting in a dynamic **ZnOEPL** complex. With three orders of magnitude larger binding constant ($K_{bind} \sim 10^6$–$10^7$ M$^{-1}$) the Ru–N bond should be stronger, making the **RuOEP(CO)L** complex more stable. Therefore, one possible explanation for the faster SET in the ruthenium complexes could be that the through bond SET is greater in the stronger bonding ruthenium complex.[37,60,61] With the longer ligands, however, where the porphyrin anthracene separation is large, close to 25 Å, it is expected that FRET is the dominating SET mechanism. Therefore, considering FRET, the faster SET could imply that the ligand can move away from the 90° binding angle to a larger extent in the ruthenium case, as schematically described in Fig. 6. A greater deviation from the 90° binding angle results in a more favourable geometry for FRET. For a detailed discussion on the angle dependence the reader is referred to ref. 25. In short, an apparent binding angle can be estimated based on the fluorescence quenching experiments and a known spectral overlap.[25] For the **RuOEP(CO)L** complexes we estimate an
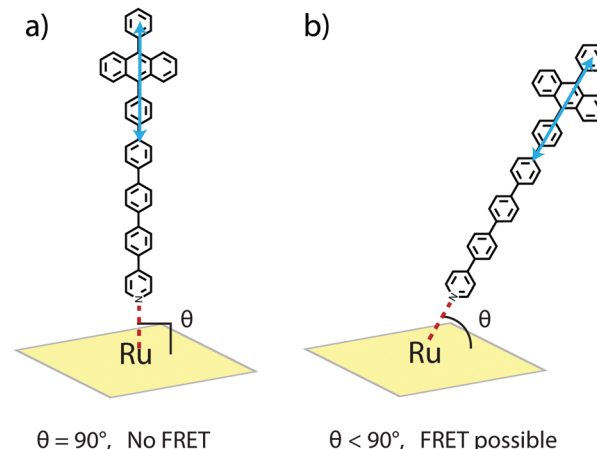


**Fig. 6** Schematic illustration of an axially coordinated ruthenium–anthracene complex with (a) perpendicular binding and (b) non-perpendicular binding, relative to the porphyrin plane and anthracene transition dipole moment. In the studied systems movement is expected and only an apparent binding angle can be estimated from the FRET measurements.

apparent binding angle of 45°, compared to >70° in **ZnOEPL**.[25] We find this large difference, however, highly unlikely, especially considering the stronger ruthenium–pyridine bond, possibly indicates that another process is also involved.

Based on the experimental results described above we can construct an energy level diagram for the **RuOEP(CO)L** complexes, as shown in Fig. 7. From the Marcus–Rehm–Weller equation, we estimate the energy of the charge separated state (**RuOEP$^+$(CO)L$^-$**) to about 2.49 eV, for details of the calculation the reader is referred to the ESI.† The energy is estimated from redox potentials in acetonitrile and should therefore be considered
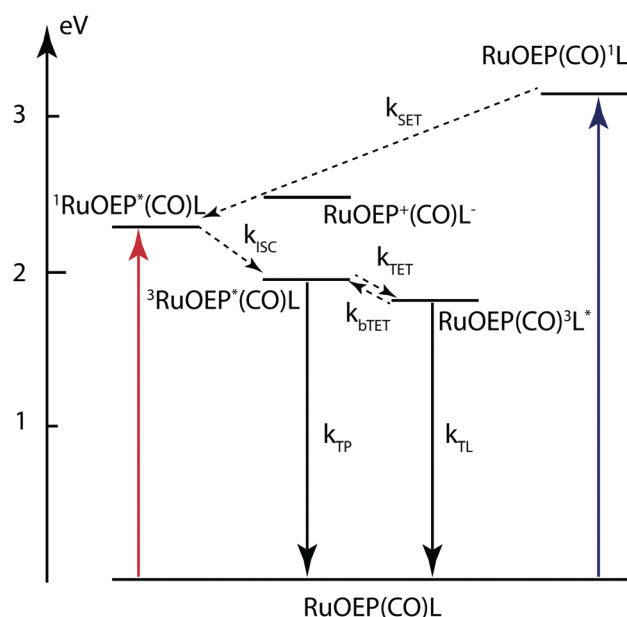


**Fig. 7** Energy level diagram of **RuOEP(CO)L** complexes. The charge separated state **RuOEP$^+$(CO)L$^-$** at 2.49 eV is estimated from the redox potentials of the free components in acetonitrile and should therefore be considered a lower limit.

**7554** | *Phys. Chem. Chem. Phys.*, 2018, **20**, 7549–7558

This journal is © the Owner Societies 2018

as a lower limit since the current systems are studied in less polar toluene. As can be seen in Fig. 7 the energy of the charge separated state is accessible from the ligand singlet state **RuOEP(CO)$^1$L\***. If populated, it would also contribute to the singlet quenching. Comparing the experimental quenching rates to a FRET governed distance dependence a reasonable $R^6$ dependence is followed as seen when comparing the slope 6 in the log–log plot in Fig. S12 (ESI†) to the experimental values. However, the best linear fit is obtained for a slightly smaller slope of 5.4, possibly indicating that there is also another factor influencing the singlet quenching.

## 1.5 RuOEP(CO)–ligand complexes applied to triplet–triplet annihilation photon upconversion

Recently, many metallo-porphyrins have been used in sensitized triplet–triplet annihilation based photon upconversion (TTA-UC) systems. In TTA-UC systems the porphyrin triplet sensitizes an annihilator molecule through TET, the triplet excited annihilator can then undergo triplet–triplet annihilation (TTA) with another triplet excited annihilator forming a singlet excited annihilator which can emit a high energy photon. The most popular porphyrins for TTA-UC are based on palladium and platinum,[20] probably due to their high intersystem crossing (ISC) yield, phosphorescent nature and stable structure. To the best of our knowledge, no ruthenium based porphyrins have been used as sensitizers for TTA-UC, even though they also have high ISC yields.[54]

One of the main challenges faced in the field of TTA-UC is the development of solid state materials that maintain the high efficiencies observed in the liquid systems. The difficulty arises from the diffusion limited TET and TTA processes which are reduced in most solid systems. One approach is to develop large supra-molecular structures where TET and TTA can occur intra-molecularly, overcoming the diffusion limit.[26] In such a supra-molecular system the sensitizer must be in close proximity to an annihilator. One advantage of ruthenium porphyrins, compared to the palladium and platinum analogues, is that pyridine ligands can coordinate to the ruthenium atom. By designing ligands that can accept the triplet energy, as described herein, the triplet energy transfer can be enhanced. We therefore used the **RuOEP(CO)L** complexes as sensitizers for TTA-UC with free DPA as an annihilator in toluene. It should be pointed out that the **RuOEP(CO)L** complexes are specifically designed to study the TET, thus TTA still must occur between two free annihilators, sensitized by two distinct complexes for upconversion to occur. As such the studied systems are only one part of a potential supra-molecular structure also incorporating intra-molecular TTA.[62]

As can be seen in Fig. 8, when **RuOEP(CO)2** is used as a sensitizer, the upconversion quantum yield, $\Phi_{UC}$, is increased about 3 times to about 4.5%,¶ compared to **RuOEP(CO)Pyr** which has $\Phi_{UC} = 1.5\%$. The quantum yields are determined in

---

¶ All reported upconversion quantum yields are on the basis of a maximum of 50%, two absorbed low energy photons can at most produce one high energy photon.
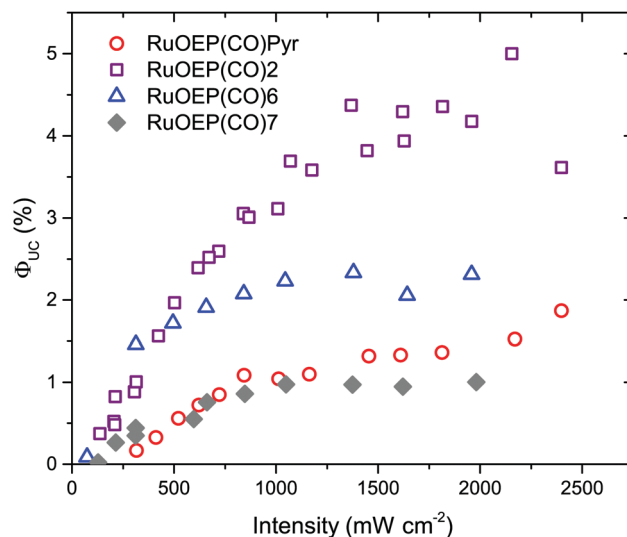


**Fig. 8** Photon upconversion quantum yield, $\Phi_{UC}$, as a function of excitation intensity. Purple squares represent samples containing **RuOEP(CO)2**, blue triangles **RuOEP(CO)6**, grey diamonds **RuOEP(CO)7** and red circles **RuOEP(CO)Pyr** as the sensitizer complex (19 μM, porphyrin/ligand 1:1), 9,10-diphenylanthracene (DPA, 0.1 mM) is added as the annihilator. All samples in toluene, prepared in a glovebox (<0.1 ppm O$_2$ and excited at 532 nm).

the strong annihilation limit (linear regime), Fig. S13 (ESI†). The increase in $\Phi_{UC}$ can be understood in terms of the extended triplet lifetime of the **RuOEP(CO)2** complex. Fig. S14 and the corresponding section in the ESI† describe the effect on the TET efficiency and $\Phi_{UC}$ by extending the triplet lifetime of the sensitizer. With the current annihilator concentration it is expected that **RuOEP(CO)2** is approximately 1.5–2 times more efficient due to the increased TET efficiency, in line with our experimental observations.

Interestingly the effect of the extended triplet lifetime is not observed to the same extent for the complexes with dendrimeric ligands, **RuOEP(CO)6** ($\Phi_{UC} = 2.3\%$) and **RuOEP(CO)7** ($\Phi_{UC} = 1.0\%$), Fig. 8. $\Phi_{UC}$ decreases more for the larger dendrimers. One possible explanation, in line with the observed decrease in $\Phi_{UC}$, is a steric effect on the probability of free DPA colliding with the triplet excited monomer in the dendrimer ligand. This is a result of the current upconversion system still relying on diffusional TET and TTA. In fully supra-molecular structures where an annihilator dendrimer is coordinated to multiple sensitizers, allowing for both TTA and TET to occur intra-molecularly we envision that such problems can be circumvented.

## 2 Conclusion

Herein we report a comprehensive study of the energy transfer processes of seven new ruthenium porphyrin–anthracene coordination complexes, **RuOEP(CO)L**. The design and synthesis of pyridine containing anthracene ligands with various bridge lengths (8–25 Å), consisting of **1–7** anthracene units, is described. The anthracene ligands bind strongly to the ruthenium atom

resulting in close to quantitative binding for a 1 : 1 mixing ratio. Upon excitation of **RuOEP(CO)** the formed triplet is quickly transferred to the axially coordinated anthracene derivative. By separating the anthracene and porphyrin with phenyl bridges we observe a decrease in the triplet energy transfer rate, and an attenuation factor $\beta$ of 0.64 Å$^{-1}$ is determined. We further study the singlet energy transfer from the anthracene ligand to **RuOEP(CO)** using ps-resolved fluorescence lifetime measurements. The singlet anthracene is readily quenched by the porphyrin. By employing large dendrimeric structures or longer phenyl bridge separators the quenching is reduced. The singlet quenching follows a Förster type $R^6$ distance dependence, even though the transition dipole moments are close to perpendicularly oriented.

The current study is part of our broader investigation of supramolecular structures for TTA based photon upconversion. Here we demonstrate that by effectively extending the triplet lifetime of the ruthenium complex by coordination of the anthracene ligands, the upconversion quantum yield is increased threefold to 4.5% with complex **RuOEP(CO)2**. We have previously studied the properties of DPA based dendrimers and oligomers[45,62] and shown that intra-molecular TTA is possible in such structures. Combined with the current study, where efficient intra-molecular TET is achieved, we are en route to developing fully functioning, well defined, supramolecular TTA upconversion systems, with broad implications spanning solar energy harvesting devices to bioimaging and drug targeting.

## 3 Experimental

Synthetic procedures for the new ligands **1**, **6** and **7**, and NMR spectra are found in the ESI.†

### 3.1 Photophysical characterization

Steady-state absorption was recorded on a Cary 5000 spectrophotometer and steady state emission measurements were carried out on a Spex Flurolog 3 spectrofluorimeter (JY Horiba). Phosphorescence decays were carried out on the mentioned spectrofluorimeter. Unquenched fluorescence lifetimes were determined on a time correlated single photon counting (TCSPC) setup using a 377 nm laser diode (PicoQuant) and a MCP-PMT detector (10 000 counts in the top channel, 2048 channels). Quenched fluorescence lifetimes were determined by time resolved emission measurements which were taken with a streak camera system; excitation pulses were generated using a Tsunami Ti:sapphire laser (Spectra-Physics) that was pumped by a Millennia Pro X laser (Spectra-Physics). The Tsunami laser output was set to 740 nm and frequency doubled to 370 nm using a frequency doubler/tripler (GWU, Spectra Physics) to excite the anthracene ligands. The emitted photons were passed through a spectrometer (Acton SP2300, Princeton Instruments) and were detected using a streak camera (C5680, Hamamatsu) with a synchroscan sweep unit (M5675, Hamamatsu).

Nanosecond transient absorptions measurements were performed on a home built system with a Surelite Continuum

Nd:YAG laser equipped with an Surelite Continuum OPO generating a 7 ns pump beam. A quartz-halogen lamp with a monochromator was used for the probe light. Either a CCD camera (iStar, Andor Technology) or a monochromator (Oriel Cornerstone 130, Newport) together with a 5 stage PMT (Applied Photophysics) coupled to an oscilloscope (TDS 2022, Tektronix) was used for recording the transient spectra or decay signal, respectively.

Upconversion samples were excited at 532 nm using a frequency doubled cw Nd:YAG laser (Millenia V, Spectra-Physics), the excitation intensity was varied using a neutral density filter and the intensity was measured using a power-meter from Starlite Ophir. The laser spot diameter was determined to be 2.5 mm using a laser alignment paper. The emission was recorded at a 90° angle by out-coupling the emission with an optical fibre to an AvaSpec 2048 (Avantes) USB fibre spectrometer with a 532 nm notch filter between the sample and the fibre to protect the spectrometer from the intense scattered excitation light.

All photophysical measurements were carried out in toluene using quartz cuvettes. Samples were prepared in a glovebox from Innovative Technologies (<0.1 ppm $O_2$) under a nitrogen atmosphere. **RuOEP(CO)L** phospohorescence quantum yields were determined using relative Cresyl violet in methanol ($\Phi$ = 54%). Upconversion quantum yields, $\Phi_{UC}$, were also determined using relative Cresyl violet in methanol employing the standard equation for relative fluorescence quantum yield determination:

$$\Phi_{UC} = \Phi_r \frac{\left(1 - 10^{-A_r}\right)}{\left(1 - 10^{-A_x}\right)} \frac{F_x}{F_r} \frac{I_r}{I_x} \frac{\eta_x^2}{\eta_r^2} \tag{6}$$

where $A$ is the absorbance, $F$ the corrected integrated emission, $I$ is the excitation intensity and $\eta$ is the refractive index of the medium. Subscripts x and r denote the sample and reference respectively.

## Conflicts of interest

There are no conflicts of interest to declare.

## Acknowledgements

## References

1 M. F. Perutz, H. Muirhead, J. M. Cox and L. C. G. Goaman, *Nature*, 1968, **219**, 131–139.

2 G. McDermott, S. M. Prince, A. A. Freer, A. M. Hawthonthwaite-Lawless, M. Z. Papiz, R. J. Cogdell and N. W. Isaacs, *Nature*, 1995, **374**, 517–521.

3 T. Mirkovic, E. E. Ostroumov, J. M. Anna, R. van Grondelle and G. D. Scholes, *Chem. Rev.*, 2017, **117**, 249–293.

4 M. R. Wasielewski, *Chem. Rev.*, 1992, **92**, 435–461.

5 D. Gust, T. A. Moore and A. L. Moore, *Acc. Chem. Res.*, 1993, **26**, 198–205.

6 D. Gust, T. A. Moore and A. L. Moore, *Acc. Chem. Res.*, 2001, **34**, 40–48.

7 G. Kodis, P. A. Liddell, L. D. Garza, P. C. Clausen, J. S. Lindsey, A. L. Moore, T. A. Moore and D. Gust, *J. Phys. Chem. A*, 2002, **106**, 2036–2048.

8 Y. Nakamura, I. W. Hwang, N. Aratani, T. K. Ahn, D. M. Ko, A. Takagi, T. Kawai, T. Matsumoto, D. Kim and A. Osuka, *J. Am. Chem. Soc.*, 2005, **127**, 236–246.

9 D. Gust, T. A. Moore and A. L. Moore, *Acc. Chem. Res.*, 2009, **42**, 1890–1898.

10 K. Gao, L. Li, T. Lai, L. Xiao, Y. Huang, F. Huang, J. Peng, Y. Cao, F. Liu, T. P. Russel, R. A. J. Janssen and X. Peng, *J. Am. Chem. Soc.*, 2015, **137**, 7282–7285.

11 S. Mathew, N. A. Astani, B. F. E. Curchod, J. H. Delcamp, M. Marszalek, J. Frey, U. Rothlisberger, M. K. Nazeeruddin and M. Grätzel, *J. Mater. Chem. A*, 2016, **4**, 2332–2339.

12 P. Qin, P. Sanghyun, M. I. Dar, K. Rakstys, H. Elbatal, S. A. Al-muhtaseb, C. Ludwig and M. K. Nazeeruddin, *Adv. Funct. Mater.*, 2016, **26**, 5550–5559.

13 J. Schmitt, V. Heitz, A. Sour, F. Bolze, H. Ftouni, J.-F. Nicoud, L. Flamigni and B. Ventura, *Angew. Chem., Int. Ed.*, 2015, **54**, 169–173.

14 G. Sedghi, K. Sawada, L. J. Esdaile, M. Hoffmann, H. L. Anderson, D. Bethell, W. Haiss, S. J. Higgins and R. J. Nichols, *J. Am. Chem. Soc.*, 2008, **120**, 8582–8583.

15 G. Sedghi, V. M. García-Suárez, L. J. Esdaile, H. L. Anderson, C. J. Lambert, S. Martín, D. Bethell, S. J. Higgins, M. Elliot, N. Bennett, J. E. Macdonald and R. J. Nichols, *Nat. Nanotechnol.*, 2011, **6**, 517–523.

16 Z. Li, T.-H. Park, J. Rawson, M. J. Therien and E. Borguet, *Nano Lett.*, 2012, **12**, 2722–2727.

17 G. Sedghi, L. J. Esdaile, H. Anderson, S. Martin, D. Bethell, S. J. Higgins and R. J. Nichols, *Adv. Mater.*, 2012, **24**, 653–657.

18 T. N. Singh-Rachford and F. N. Castellano, *Coord. Chem. Rev.*, 2010, **254**, 2560–2573.

19 J. Zhao, S. Ji and H. Guo, *RSC Adv.*, 2011, **1**, 937–950.

20 V. Gray, D. Dzebo, M. Abrahamsson, B. Albinsson and K. Moth-Poulsen, *Phys. Chem. Chem. Phys.*, 2014, **16**, 10345–10352.

21 C. E. McCusker and F. N. Castellano, *Top. Curr. Chem.*, 2016, **374**, 19.

22 T. G. Monger, R. J. Cogdell and W. W. Parson, *Biochim. Biophys. Acta*, 1976, **449**, 136–153.

23 A. Gall, R. Berera, M. T. A. Alexandre, A. A. Pascal, L. Bordes, M. M. Mendes-pinto, S. Andrianambinintsoa, K. V. Stoitchkova, A. Marin, L. Valkunas, P. Horton, J. T. M. Kennis, R. V. Grondelle, A. Ruban and B. Robert, *Biophys. J.*, 2011, **101**, 934–942.

24 J. Ho, E. Kish, D. D. Méndez-Hernández, K. WongCarter, S. Pillai, G. Kodis, J. Niklas, O. G. Poluektov, D. Gust, T. A. Moore, A. L. Moore, V. S. Batista and B. Robert, *Proc. Natl. Acad. Sci. U. S. A.*, 2017, **114**, E5513–E5521.

25 V. Gray, K. Börjesson, D. Dzebo, M. Abrahamsson, B. Albinsson and K. Moth-Poulsen, *J. Phys. Chem. C*, 2016, **120**, 19018–19026.

26 C. Fan, W. Wu, J. J. Chruma, J. Zhao and C. Yang, *J. Am. Chem. Soc.*, 2016, **138**, 15405–15412.

27 N. Yanai and N. Kimizuka, *Chem. Commun.*, 2016, **52**, 5354–5370.

28 F. Li, Y. Jiang, B. Zhang, F. Huang, Y. Gao and L. Sun, *Angew. Chem., Int. Ed.*, 2012, **51**, 2417–2420.

29 J. Liu, L. Chen, H. Cui, J. Zhang, L. Zhang and C.-Y. Su, *Chem. Soc. Rev.*, 2014, **43**, 6011–6061.

30 V. Bandi, F. P. D. Souza, H. B. Gobeze and F. D'Souza, *Chem. – Eur. J.*, 2015, **21**, 2669–2679.

31 K. Kilså, J. Kajanus, S. Larsson, A. N. Macpherson, J. Mårtensson and B. Albinsson, *Chem. – Eur. J.*, 2001, **7**, 2122–2133.

32 D. Holten, D. F. Bocian and J. S. Lindsey, *Acc. Chem. Res.*, 2002, **35**, 57–69.

33 A. Prodi, C. Chiorboli, F. Scandola, E. Iengo, E. Alessio, R. Dobrawa and F. Würtner, *J. Am. Chem. Soc.*, 2005, **127**, 1454–1462.

34 D. M. Guldi, G. M. A. Rahman, V. Sgobba and C. Ehli, *Chem. Soc. Rev.*, 2006, **35**, 471–487.

35 Y. Nakamura, N. Aratani and A. Osuka, *Chem. Soc. Rev.*, 2007, **36**, 831–845.

36 B. Albinsson, M. P. Eng, K. Pettersson and M. U. Winters, *Phys. Chem. Chem. Phys.*, 2007, **9**, 5847–5864.

37 B. Albinsson and J. Mårtensson, *J. Photochem. Photobiol., C*, 2008, **9**, 138–155.

38 T. K. Khan, M. Bröring, S. Mathur and M. Ravikanth, *Coord. Chem. Rev.*, 2013, **257**, 2348–2387.

39 J. G. Woller, J. K. Hannestad and B. Albinsson, *J. Am. Chem. Soc.*, 2013, **135**, 2759–2768.

40 M. Gilbert and B. Albinsson, *Chem. Soc. Rev.*, 2015, **44**, 845–862.

41 A. Antoniuk-Pablant, G. Kodis, A. L. Moore, T. A. Moore and D. Gust, *J. Phys. Chem. B*, 2016, **120**, 6697.

42 H. Dekkiche, A. Buisson, A. Langlois, P.-L. Karsenti, L. Ruhlmann, P. D. Harvey and R. Ruppert, *Inorg. Chem.*, 2016, **55**, 10329–10336.

43 D. R. Martir, G. J. Hedley, D. B. Cordes, A. M. Z. Slawin, D. Escudero, D. Jacquemin, T. Kosikova, D. Philp, D. M. Dawson, S. E. Ashbrook, I. D. W. Samuel and E. Zysman-colman, *Dalton Trans.*, 2016, **45**, 17195–17205.

44 Y. Hu, M. B. Thomas, R. G. W. Jinadasa, H. Wang and F. D'Souza, *Chem. – Eur. J.*, 2017, **23**, 12805–12814.

45 K. Börjesson, M. Gilbert, D. Dzebo, B. Albinsson and K. Moth-Poulsen, *RSC Adv.*, 2014, **4**, 19846.

46 M. Tsutsui, D. Ostfeld and L. M. Hoffman, *J. Am. Chem. Soc.*, 1971, **93**, 1820–1823.

47 A. Antipas, J. W. Buchler, M. Gouterman and P. D. Smith, *J. Am. Chem. Soc.*, 1978, **100**, 3015–3024.

48 D. P. Rillema, J. K. Nagle, L. F. Barringer Jr and T. J. Meyer, *J. Am. Chem. Soc.*, 1981, **103**, 56–62.

49 K. M. Kadish, D. J. Leggett and D. Chang, *Inorg. Chem.*, 1982, **21**, 3618–3622.

This journal is © the Owner Societies 2018

*Phys. Chem. Chem. Phys.*, 2018, **20**, 7549–7558 | 7557

50 K. M. Kadish and D. Chang, *Inorg. Chem.*, 1982, **21**, 3614–3618.

51 S. Chattopadhyay, C. V. Kumar and P. Das, *Chem. Phys. Lett.*, 1983, **98**, 250–254.

52 V. Gray, D. Dzebo, A. Lundin, J. Alborzpour, M. Abrahamsson, B. Albinsson and K. Moth-Poulsen, *J. Mater. Chem. C*, 2015, **3**, 11111–11121.

53 J. Andraos, *J. Chem. Educ.*, 1999, **76**, 1578–1583.

54 L. M. A. Levine and D. Holten, *J. Phys. Chem.*, 1988, **92**, 714–720.

55 J. Vura-Weis, S. H. Abdelwahed, R. Shukla, R. Rathore, M. A. Ratner and M. R. Wasielewski, *Science*, 2010, **328**, 1547–1550.

56 N. I. Nijegorodov, W. S. Downey and M. B. Danailov, *Spectrochim. Acta, Part A*, 2000, **56**, 783–795.

57 E. A. Weiss, M. J. Ahrens, L. E. Sinks, A. V. Gusev, M. A. Ratner and M. R. Wasielewski, *J. Am. Chem. Soc.*, 2004, **126**, 5577–5584.

58 E. A. Weiss, M. J. Tauber, R. F. Kelley, M. J. Ahrens, M. A. Ratner and M. R. Wasielewski, *J. Am. Chem. Soc.*, 2005, **127**, 11842–11850.

59 T. Mani, D. M. Niedzwiedzki and S. A. Vinogradov, *J. Phys. Chem. A*, 2012, **116**, 3598–3610.

60 K. Kilså, J. Kajanus, J. Mårtensson and B. Albinsson, *J. Phys. Chem. B*, 1999, **103**, 7329–7339.

61 K. Pettersson, A. Kyrychenko, E. Ro and T. Ljungdahl, *J. Phys. Chem. A*, 2006, **110**, 310–318.

62 D. Dzebo, K. Börjesson, V. Gray, K. Moth-Poulsen and B. Albinsson, *J. Phys. Chem. C*, 2016, **120**, 23397–23406.

7558 | *Phys. Chem. Chem. Phys.*, 2018, **20**, 7549–7558

This journal is © the Owner Societies 2018